Retrodirective Array Phase Modulation for Ultra Low-Power Communications

Gregory A Koo, *Student Member, IEEE,* Yenpao A Lu, *Student Member, IEEE,* and Gregory D Durgin, *Senior Member, IEEE*

***Abstract*—A Retrodirective Array Phase Modulator(RAPM) implements higher-order Phase Shift Keying(PSK) in a backscatter link and provides a means for ultra low power communications for RFID and wireless sensor networks. RAPM implementations consist of highly efficient FET switches and a low-power microcontroller that consumes microwatts of power. The RAPM's operation is analyzed in the forward and backward channels to show how separate signal paths combine in phase at the receiver and produce maximal gain. A RAPM prototype is constructed and its S_{21} characteristics demonstrate its PSK capability.**

***Index Terms*—Retrodirective Array, Passive Switching, Remote Sensing, Backscatter.**

I. Introduction

DEVELOPED in 1955 by L.C. Van Atta, the retrodirective array (RA) holds the unique property that any impinging waveform is reradiated back toward the radiating source [1]. Unlike smart antennas that use active beamsteering, Van Atta's design does not require additional hardware such as phase shifters or local oscillators. Built upon his design, the RAPM with L antenna elements provides an L^2 increase in backscattered power when compared to a single antenna and is capable of performing higher-order PSK modulation. This ability to perform PSK reduces the symbol rate, and hence, operational duty cycle for the microcontroller that drives the communication of the retrodirective array. The operational range of a passive backscatter sensor was shown to greatly improve as duty cycle decreased[2]. Smith et al demonstrated that for the WISP architecure, the read range of an RF tag more than doubled when the microcontroller duty cycle was 1/9th. The channel coefficients for the foward and backward links of the retrodirective array also combine to remove phase differences between separate signal paths, increasing gain and providing a maximal Signal-to-Noise Ratio (SNR) at the receiver. Such traits provide tremendous benefit for backscatter radio operation, which suffers from low backscattered power levels and a radar-like link budget[3].

Yet Van Atta's design is not the only option for achieving retrodirectivy. There are also two other classes of retrodirective arrays shown in Figure 1, the well known corner reflector and the Pon array. The corner reflector benefits from completely passive retrodirectivity, but is severly lacking due to a non planar structure, bulky size at microwave frequencies, and no active communication ability. The array proposed by C.Y. Pon in 1964 however, is capable of communication. The Pon array, commonly known as a heterodyne array, utilizes a common LO source and a mixer at each antenna element to produce the conjuate phase shift required to reradiate a signal back toward the source [4]. These two components also provide the array with the ability to perform both up and downconversion [5]. Another means of communication involves a Maxwellian lens with diametrically placed antennas and impedance modulating pin diodes[6]. Power of the reradiated signal in an RA can also be boosted by using inline amplifiers, as demonstrated by Chung, who was able to achieve a 4.5 dB gain in backscattered field magnitude [7]. By biasing the inline amplifiers between their on and off states, an on-off keying communication scheme can also be employed .[8].

The latter retrodirective array implementations, however, draw power in the range of ten's of milliamps or more, making passive backscatter operation unfeasible in the far field. The RAPM design proposed in this paper overcomes the power consumption problem by implementing efficient GaAs FET switches and an onboard microcontroller. In doing so, the power draw for a four element array is kept below 1mW, an order of magnitude less than competing architectures . The proposed design implements QPSK modulation to further increase the design's efficiency; since only the phase of the reradiated signal is being manipulated, no inline amplifiers, pin diodes, or amplitude modulators are required, immediately eliminating a substantial amount of power draw.

II. Retrodirective Array Operation

To provide an understanding of how retrodirectivity occurs, a brief analyis showing the interaction between a RA and an incident wavefront is presented. Figure 1 shows a basic four element linear equally spaced RA constructed with identical antennas that are mirrored with respect to the centroid, or inversion point of symmetry, of the array. Beginning with the inner antenna pair, an arbitrary length transmission line is connected between the two radiating elements. Each additional antenna pair must then be connected by a transmission line of length d or $d + n\lambda$, where n is a positive, real integer. This constraint arises from the need to maintain the relative phase offset that occcurs between each antenna when an oblique wavefront impinges upon the array. Without these electrically identical lengths, undesired interference occurs when the wave is reradiated and retrodirectivity no longer holds. Shown at the top of Figure 1, an impinging wave encounters the first antenna element. The phase difference at the other antenna elements

G. Koo is with the Department of Electrical and Computer Engineering, Georgia Institute of Technology, Atlanta,GA 30332 USA

4

Fig. 1. 4-Element retrodirective array (Top), Pon array (Bottom Left), Corner reflector (Bottom Right)

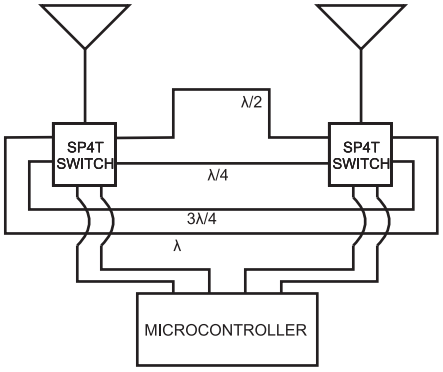

Fig. 2. Schematic of a two element retrodirective array phase modulator; Microcontroller simulataneously controls switches to change phase length of transmission line between antenna pair.

can be shown as

$$\phi_{diff} = \frac{2\pi \cdot \sin(\theta) ad}{\lambda_0} \tag{1}$$

,where θ is the angle of incidence w.r.t broadside, a is the antenna index of the array, as shown in Figure 1, and d is the spacing between antenna elements. As the antennas on the right side of the array absorb the impinging wave, relative phase differences are maintained as the waves propagate down the lines connecting each antenna pair. These travelling waves are then reradiated by the antennas to the left of the array's inversion center. The reciprocal process occurs after the incident wave crosses the inversion center of array. In the case of Figure 1, the wave is absorbed by antennas 1 and 2 and reradiated by antennas 4 and 3, respectively. Antennas 3 and 4 then absorb the wavefront at a later point in time, and antennas 2 and 1 reradiate the wave. After this complete cycle, a uniform wavefront with a conjugate phase propagates back toward the radiating source.

A. RAPM Operation

The phase of an absorbed wavefront can be altered by selecting different line lengths to connect between antenna pairs, as shown in the QPSK RAPM of Figure 2. By controlling the FET switches simulataneously via a microcontroller, one can achieve M-ary phase shift keying of the reradiated wave. To construct an L element RAPM, each antenna pair requires its own pair of switches and tranmission lines. Only one microcontroller is needed in a QPSK setup though, since the FETs for all antenna pairs must be switch to the same line length, allowing them to driven in parallel off a single 8-bit i/o bus.

B. Backscatter Signalling Matrix

To characterize the RAPM further, a general backscatter signalling matrix, shown in Equation 2, was derived from two-port scattering theory for a lossless, reciprocal RAPM.

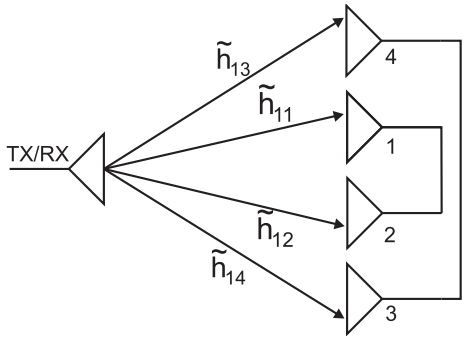

Fig. 3. Foward channel for 4 element RAPM using baseband channel coefficients. The backward channel consists of the same diversity branches with conjugate phases.

$$\bar{S}(t) = \begin{bmatrix} P & 0 & 0 & 0 & 0 & \cdots \\ 0 & 0 & P & 0 & 0 & \\ 0 & P & 0 & 0 & 0 & \\ 0 & 0 & 0 & 0 & P & \\ 0 & 0 & 0 & P & 0 & \\ \vdots & & & & \ddots & \end{bmatrix} \text{,where} P = e^{-j\frac{2\pi}{\lambda}\ell(t)} \tag{2}$$

Within the phase term, P, ℓ(t) represents the different line lengths that can be interchanged as function of time. For the specific QPSK scenario, ℓ(t) can be λ/4, λ/2, 3λ/4, or λ, resulting in a signal constellation with 90° phase rotations between the four different states. For an odd number of antenna elements, the antenna at the inversion center becomes port 1. The next innermost antenna pair becomes ports 2 and 3, etc. Note that since the antenna pair network is reciprocal, $\bar{S}(t) = \bar{S}(t)^t$, and it is arbitrary to select which antenna corresponds to port 2 or port 3. Thus the elements in the signalling matrix at indices 2,3 and 3,2 characterize the phase shift that occurs as the absorbed wave propagates between an antenna pair. This genreral $L \times L$ scattering matrix applies to any two or three dimensional retrodirective array with L antenna elements. If the number of array elements is even, the signalling matrix remains symmetric, but the first column and row are removed from Equation 2. For this case, shown in Figure 3, the innermost antenna pair is labeled with port numbers 1 and 2, and P terms would result at the 1,2 and 2,1 indices in $\bar{S}(t)$.

C. Channel Properties

The gain increase created by the RAPM can be explained through the general $M \times L \times N$ dyadic backscatter channel model, where M, L, and N represent the number of antennas at the transmitter, RAPM, and receiver. The general model can be simplified to $1 \times L \times 1$, since the reradiated signal is directed back toward the transmit antenna. Also known as a monostatic configuration, the $1 \times L \times 1$ case implements a single antenna to transmit and receive. Under monostatic conditions, the forward channel can be depicted as in Figure 3. Each array element is assigned a unique channel coefficent since individual diversity branches arise from spatial separation of the antennas. To

determine the backward channel coeffecients, the conjugates of the forward coefficients are taken. The tranmission of a signal $\tilde{x}(t)$ through the baseband equivalent channel can then by described by Equation 3. For a more detailed analysis, see references[9] and [10].

$$\tilde{y}(t) = \frac{1}{2}\tilde{\vec{h}}^{b}(\vec{r})\bar{S}(t)\tilde{\vec{h}}^{f}(\vec{r})\tilde{x}(t) + \tilde{n}(t) \tag{3}$$

In equation 3, the physical channel convention was taken to relate the channel coeffecients to voltage measured at the receive antenna's terminals. For the monstatic case, $\tilde{x}(t)$ and $\tilde{n}(t)$ become scalar. $\bar{S}(t)$ is the $L \times L$ signalling matrix, and $\tilde{\vec{h}}^{b}(\vec{r})$ and $\tilde{\vec{h}}^{f}(\vec{r})$ are vectors of dimension L. Invoking the local area approximation, the general form of $\tilde{\vec{h}}^{f}(\vec{r})$ becomes

$$\tilde{\vec{h}}^{f}(\vec{r}) = \tilde{h}_0 \begin{bmatrix} e^{-j\frac{2\pi}{\lambda_0}\hat{k}\cdot\vec{r}_1} \\ e^{-j\frac{2\pi}{\lambda_0}\hat{k}\cdot\vec{r}_2} \\ \\ \vdots \\ e^{-j\frac{2\pi}{\lambda_0}\hat{k}\cdot\vec{r}_L} \\ \\ \end{bmatrix} \tag{4}$$

, where $\tilde{h}_0$ represents channel's effect upon the amplitude and phase of $x(t)$. The $e^{-jk_0\hat{k}\cdot\vec{r}}$ terms represent phase differences at each RAPM antenna with respect to the inversion point of symmetry for an incident plane wave. The distance vectors, $\vec{r}$, whose subscripts correspond to the port numbers assigned during the creation the signalling matrix, are simply vectors from the inversion point of symmetry to each antenna's feed port.

From equation 4, one can create the $\tilde{\vec{h}}^{b}(\vec{r})$ row vector by taking the transpose of the forward channel coefficient, $\tilde{\vec{h}}^{f}(\vec{r})$. The following simplifications can then applied to Equation 3 to demonstrate the L^2 power gain associated with the RAPM. We begin by letting the noise component go to zero, normalizing $\tilde{y}(t)$ by $\frac{1}{2}\tilde{h}_0$, and making $\tilde{x}(t)$ be of constant amplitude and unity magnitude. Then since

$$\bar{S}(t)\tilde{\vec{h}}^{f}(\vec{r}) = \tilde{\vec{h}}^{f}(\vec{r})^{*}, \tag{5}$$

and

$$\tilde{\vec{h}}^{f}(\vec{r}) = \tilde{\vec{h}}^{b}(\vec{f})^{t} \tag{6}$$

, equation (6) may be substituted into equation (5) to get $\tilde{y}(t)$ solely in terms of $\tilde{\vec{h}}^{b}(\vec{f})$. $\tilde{y}(t)$ then simplifies to be the norm of the backward channel coefficient, $\tilde{\vec{h}}^{b}(\vec{r})$, and $\tilde{y}(t)$ is shown to depend on L.

$$\tilde{y}(t) = \tilde{\vec{h}}^{b}(\vec{r})\tilde{\vec{h}}^{b}(\vec{r})^{\dagger} = L \tag{7}$$

This resulting baseband output for the backscatter channel shows a maximal gain and a received voltage and power proportional to L and L^2, respectively. Griffin et al. demonstrated that in addition to the SINR gain provided by the increased effective scattering aperature for an L antenna RF tag, pinholde diversity gains also occured. For a $1 \times L \times 1$ configuration, a total SINR increase of up to 10dB at 10^{-4} BER for uncoded BPSK and rayleigh fading was shown [10].

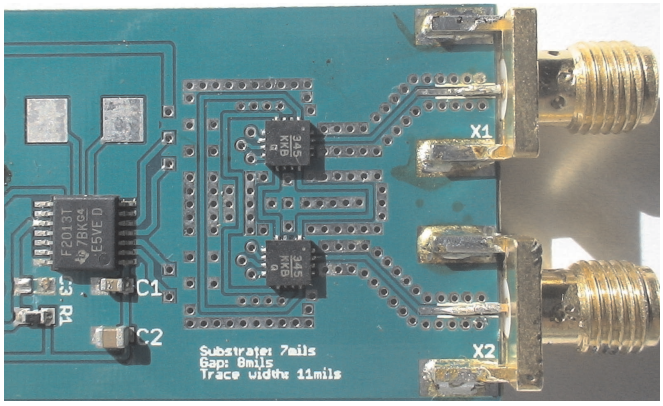

Fig. 4. Two element RAPM board constructed on FR4 with an TI MSP430F2013 microcontroller and two Hittite HMC345LP3 SP4T switches.

Similar improvements for pinhole diversity gains would be expected for the RAPM, since each array element acts as a pinhole in the channel.

III. Design of Retrodirective Array Phase Modulator (RAPM)

A. Board Design

A QPSK RAPM prototype was constructed on a 4-layer FR4 substrate with an ϵ_r=5.2, trace width of 11 mils and a gap of 8 mils to verify the phase shifting capability of the switching circuitry. Two Hittite HMC345LP3 GaAs switches were controlled by a TI MPS430F2013 microcontroller. Figure 4 shows the 2-element prototype. The common RF ports of the switches were connected to SMA connectors to allow network analyzer characterization as well as arbitrary antenna attachement.

IV. Results

The RAPM prototype's phase shifting capabilites were observed by measuring its S_{21} parameters with an Agilent E5071B network analyzer set to a 0 Hz span. The microcontroller was programmed to repeatedly switch between transmission lines in the following sequence: λ/4, λ/2, 3λ/4, and λ. The switching frequency was chosen to be 1-kHz to represent the low data rates common in remote sensing, but the microcontroller is capable of operating at 10 Msymbols/sec for burst mode transmissions. As shown in Figure 5, the 90° phase shifts between the four states demonstrates the ability of the RAPM to perform QPSK. The exact relative phase differences between the four states of the RAPM were measured to be: 88.3°, 79.2°, 98.16°,and 94.33°.

It can be shown through either the backscatter link budget equation or a channel anlysis that the maximum power received at an interrogator when using an L element RAPM is L^2 greater than the power received by a single antenna device. When peforming link budget analysis for a RAPM implemention, the following equation can then be used,

$$P_r^{RAPM} = L^2 \cdot P_r^{SingleAntenna} \tag{8}$$

where the P_r terms represent the power received in a backscatter link budget.

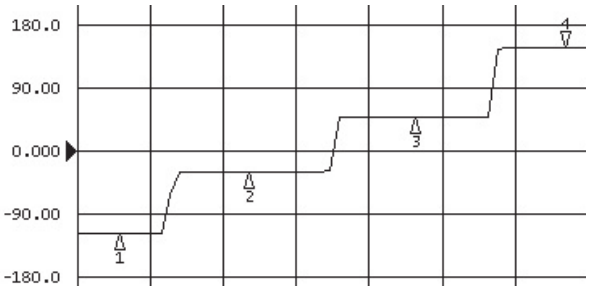

Fig. 5. S_{21} measurent of phase vs. time for RAPM switching rate of 1 ksymbols/sec

V. Conclusion

The RAPM provides reduced power consumption when compared to previous information carrying retrodirective array designs. By taking Van Atta's original design and incorporating a novel, passive QPSK modulation achitecture, a more efficient backscatter communication platform has been created that harnesses the power of retrodirectivity. The ability of the proposed architecture to increase the range of backscatter radio communication provides a new sector for future research and applications in the field, and with sub-milliwatt power requirements, the design has potential to become a realizable option over conventional backscatter communication hardware.

References

[1] L. C. Van Atta, "Electromagnetic reflector," US Patent 2,908,002, October, 1959.

[2] J. R. Smith, A. P. Sample, P. S. Powledge, S. Roy, and A. Mamishev, "A wirelessly-powered platform for sensing and computation," *Ubicomp*, pp. 495–506, 2006.

[3] J. D. Griffin and G. D. Durgin, "Complete link budgets for backscatter-radio and rfid systems," *IEEE Antennas and Propgation Magazine*, vol. 51, pp. 11–25, April 2009.

[4] C. Y. Pon, "Retrodirective array using the heterodyne technique," *IEEE Transactions on Antennas and Propagation*, vol. 12, pp. 176–180, Mar. 1964.

[5] S. Lim, K. Leong, and T. Itoh, "Adaptive power controllable retrodirective array system for wireless sensor server applications," *IEEE Transactions on Mircowave Theory and Techniques*, vol. 53, pp. 3735–3743, Dec. 2005.

[6] R. J. Wohlers and S. N. Andre, "Circular retrodirective array," US Patent 3,958,246, May, 1976.

[7] S. J. Chung, S. M. Chen, and Y. C. Lee, "A novel bi-directional amplifier with applications in active van atta retrodirective arrays," *IEEE Transactions on Mircowave Theory and Techniques*, vol. 51, pp. 542–547, Feb. 2003.

[8] L. Chiu, Q. Xue, and C. H. Chan, "A wideband circularly-polarized active van atta retrodirective transponder with information carrying ability," *Proceeding of Asia-Pacific Microwave Conference*, 2006.

[9] G. D. Durgin, *Space-Time Wireless Channels*. Upper Saddle River, NJ: Prentice Hall Ptr, 2003.

[10] J. D. Griffin and G. D. Durgin, "Gains for rf tags using multiple antennas," *IEEE Transactions on Antennas and Propagation*, vol. 56, pp. 563–570, Feb. 2008.